in vivo *37*: 1052-1064 (2023)
doi:10.21873/invivo.13180

Enhancement of Wound Healing Efficacy by Chitosan-based Hydrocolloid on Sprague Dawley Rats

LINH THI THUY LE[1,2#], NGUYEN NGAN GIANG[2,3#], PHAM NGOC CHIEN[2], XUAN-TUNG TRINH[2], NGUYEN-VAN LONG[2], LE THI VAN ANH[2], PHAM THI NGA[2], XIN-RUI ZHANG[2,4], SUN-YOUNG NAM[2] and CHAN-YEONG HEO[2,3,4]

[1]*Department of Biomedical Science, College of Medicine, Seoul National University, Seoul, Republic of Korea;*
[2]*Department of Plastic and Reconstructive Surgery, Seoul National University Bundang Hospital, Seongnam, Republic of Korea;*
[3]*Department of Medical Device Development, College of Medicine, Seoul National University, Seoul, Republic of Korea;*
[4]*Department of Plastic and Reconstructive Surgery, College of Medicine, Seoul National University, Seoul, Republic of Korea*

Abstract. *Background/Aim: Chitosan-based functional materials have attracted considerable attention worldwide for applications in wound healing, especially in skin wound healing, due to their efficiency in hemostasis, anti-bacterial, and skin regeneration. Various chitosan-based products have been developed for skin wound healing applications, but most of these face limitations in either efficacy or cost-effectiveness. Therefore, there is a need to develop a unique material that can handle all of these concerns and be utilized for acute and chronic wounds. This study investigated mechanisms of new chitosan-based hydrocolloid patches in inflammatory reduction and skin formation by using wound-induced Sprague Dawley Rats. Materials and Methods: Our study combined a hydrocolloid patch with chitosan to achieve a practical and accessible medical patch that would enhance skin wound healing. Our chitosan-embedded patch has shown a significant influence by preventing wound expansion and inflammation increment on Sprague Dawley rat models. Results: The chitosan patch significantly increased the wound healing rate and accelerated the inflammatory stage by suppressing pro-inflammatory cytokines activity (e.g., TNF-α, IL-6, MCP-1, and IL-1β). Moreover, the product was effective in promoting skin regeneration, demonstrated by the increase in the number of fibroblasts through specific biomarkers (e.g., vimentin, α-SMA, Ki-67, collagen I, and TGF-β1). Conclusion: Our study on the chitosan-based hydrocolloid patches not only elucidated mechanisms of reducing inflammation and enhancing proliferation, but also provided a cost-effective method for skin wound dressing.*

The human skin provides a barrier against external influences, while functions as sensory detection, fluid homeostasis, immunological surveillance, and thermo-regulation (1, 2). When wounded, it loses effectiveness and is more susceptible to pathogenic diseases. Typically, the body may repair damaged skin through a multiphase, multifactorial process that requires favorable conditions. Hemostasis, inflammation, proliferation, and skin remodeling are the four steps of this physiological wound-healing mechanism (3, 4). During the hemostasis stage, following blood vessel constriction and platelet aggregation, the coagulation system becomes active. Insoluble fibrin is created from fibrinogen and forms clots to control bleeding. During the inflammation stage, inflammatory cells eliminate bacteria and necrotic tissue. In the proliferation stage, epithelial cells multiply and move to develop epithelial tissue that covers the wound, and the tissue gap is filled with granulation tissue. The newly formed epidermis and dermis

[#]These Authors have contributed equally to this study.

Correspondence to: Sun-Young Nam, Ph.D., Department of Plastic and Reconstructive Surgery, Seoul National University Bundang Hospital, Seongnam, Republic of Korea. Tel: +82 1077112423, email: 99261@snubh.or; Chan-Yeong Heo, MD, Ph.D., Department of Medical Device Development, Seoul National University, Seoul, Republic of Korea. Tel: +82 317877222, email: lionheo@snu.ac.kr

Key Words: Wound healing, chitosan, inflammation, anti-inflammation, tissue regeneration.

will regenerate during the last remodeling stage to complete the skin repair process (5).

The wound healing process could be impeded by various factors; from local factors (decreased oxygen, wound infection, foreign body), to systemic factors (age and sex, low vascularization, diseases, obesity, immune deficiency) (6). When the healing process is interrupted, tissues close unsuccessfully and become chronic wounds (7). Chronic wounds are a significant and growing burden on healthcare systems that affect more than 40 million patients globally, significantly limit the workforce, and are expected to cost more than $15 billion yearly by 2022. This leads to the need to develop cost-effective wound dressing capable of establishing a moist wound environment, avoiding secondary infections, non-adherence to damaged tissues, absorbing excess exudate, and promoting tissue regeneration. Dressings should be comfortable for the patient, reduce pain, diminish scar formation, and have an extended shelf-life (8, 9). To meet these demands, different kinds of modern wound dressings have been developed such as transparent film dressing, foams dressings, hydrogels-based dressings, hydro-conductive wound dressings, and hydrocolloids (10-12). Nevertheless, currently, none of them can universally address all the requirements and be considered an ideal wound care product. For instance, transparent film dressings provide a moist environment and a barrier to external bacteria contamination, allowing gas exchange, but cannot absorb exudate, so they are unsuitable for heavily exuding wounds. Foam dressings, as opposed to transparent film dressings, have excellent liquid absorption while still can ensure thermal insulation and gas exchange (13). However, they may provoke skin irritation and maceration along the wound periphery if factors including density, thickness, tensile strength, and elongation of freeze-dried foam are not properly adjusted (14). Therefore, there is a need to develop a novel material that can address all these issues and can be used for different types of wounds, from acute to chronic.

A hydrocolloid dressing comprises two layers: an external layer of polyurethane against water, oxygen, or bacteria, and an internal layer of hydrophilic colloidal particles which absorb wound exudate and protect and promote the newly formed granulation tissue (14). Previous studies have demonstrated that hydrocolloid dressings have the ability to accelerate the healing process by enhancing autolysis and endogenous removal of necrotic tissues. In addition, the hydrocolloid external layer, in contrast to hydrogels, can more effectively cover the wound and serve as a barrier without the need for additional dressings (7). Having many advantages as a potential base material in wound healing, using hydrocolloids in conjunction with a biomaterial can reduce inflammation, promote wound healing, allowing synergistic treatment results, and enhance functionalities.

There exist many literature reports on the use of naturally-derived polymers that has bacteriostatic action and actively enhance tissue regeneration (15). Among them, chitosan and its derivatives are promising polymers for wound-healing applications due to their hemostatic, anti-bacterial, and fungistatic qualities, as well as their effectiveness in healing capacity (16, 17). Specifically, chitosan can be primarily used in the first three phases of the wound healing process. In the beginning, it aids in halting bleeding by encouraging platelet and erythrocyte aggregation and inhibiting fibrinolysis during the hemostasis stage (18). Secondly, during the inflammation stage, chitosan can assist in clearing bacteria from the wound by altering cell wall rigidity, and disrupting it (19), chelating metal ions that are beneficial to the microbial cell (20, 21), interacting with microbial DNA (22), and forming a dense polymer film on the surface of the cell to reduce the nutrient and oxygen uptake (23, 24). Finally, chitosan can encourage the release of cytokines that promote the development of granulation tissue and accelerate skin proliferation, such as TGF-β1, PDGF, and IL-1, IL-8, in the proliferation stage (25). The wound is then repaired, and the skin is remodeled to complete the healing process.

In this study, we utilized chitosan as a potential candidate to develop a brand-new hydrocolloid dressing that promotes wound healing and is suitable for numerous types of wounds. It was applied to Sprague-Dawley rat skin wounds to investigate the contribution and effect of this patch on the wound healing process by a range of immunological studies, such as immunofluorescence (IF) staining, western blots, enzyme-linked immunosorbent assay (ELISA), and hematoxylin and eosin (H&E) staining.

Materials and Methods

The Chitosan Hydrocolloids were from CGBio company (Seoul, Republic of Korea). The patch was created according to the instructions in a pending patent.

Rat skin wound healing experiments. Animal experiments were approved by the Institutional Animal Care and Use Committee of Seoul National University Bundang Hospital (approval number: BA1608-206/045-02). Nine-week-old Sprague Dawley adult male rats weighing between 200 and 350 grams were kept in groups of 2 with free food and drink accession. The rats were maintained in a controlled environment under specific-pathogen-free (SPF) conditions, with 12h light/dark cycle, relative humidity of 55%, and a temperature of 24˚C. On the day of surgery, rats were divided into two groups at random: control (n=6) and chitosan hydrocolloid (chitosan HC) (n=6).

Both groups were anesthetized with Isoflurane. An electric hair clipper shaved the dorsal hair to create the surgical region and then disinfected this with Betadine. Full-thickness excisional wounds were created by 10 mm biopsy punch-modified tools in the Sprague Dawley rat's dorsal side. For 13 days, the control group did not receive treatment, whereas the chitosan HC was applied to cover the wound of the chitosan group, and the wound was sealed by commercial film dressing every day.

Measurement of the wound area. The kinetics of wound closure was imaged with a digital camera from days 0, 3, 7 10, and 13 after all the wound dressings were removed. The percentage of wound healing was calculated by the following equation:

$$\text{Percentage of wound healing } (\%)=(A_0-A_n)/A_0\times 100\%$$

Where A_0 presents the initial wound area post-surgery (day 0), and A_n presents the wound healing area on an n^{th} day after surgery. ImageJ software was used to measure the wound area based on the photographs. The average time for wound closure was calculated using six rats from each group.

Histological analysis. On day 13, after wound healing was photographed, 6 rats in each group were sacrificed. The biopsied tissues were embedded in paraffin after being fixed in 10% formaldehyde for 24 h at 40˚C. The thicknesses of sections of 5 μm were prepared to investigate the histological analysis of the wound healing sections with different methods. The sections were stained with hematoxylin and eosin (H&E) staining to measure the granulation tissue thickness and the thickness of the epidermis. The sections were stained with MT staining for measurement of collagen fiber production and collagen intensity.

H&E staining. The tissue sections were performed by deparaffinization in xylene for 3 min with two times before rehydration in a different reducing concentration of ethanol following such as 100% ethanol for 3 min with two times, 95%, 90%, 80%, and 70% ethanol for every 3 min and finally washed with distilled water for 3 min two times. The tissue sections were stained for 5 min with Hematoxylin, rinsed in distilled water for 3 min 2 times to remove the excess stain, and then incubated for 10-15 seconds in Bluing reagent. The tissue sections were then washed with distilled water, followed by incubation in Eosin Y solution for 3 min, and dehydrated in three changes of 100% ethanol every 3 min. Finally, tissue sections were mounted with synthetic resin and coverslipped. The result of H&E staining was quantified by using a microscope.

MT staining. The staining of tissue slides was performed following the manufacturer instructions through deparaffinization and rehydration and then stained by Masson's trichrome staining kit. Specifically, tissue slides were incubated with Bouin at room temperature overnight and rinsed with distilled water until the tissue slides were completely clear. After that, tissue sections were stained with Weigert's Hemamotoxylin for 10 min, rinsed with distilled water, and immersed in Biebrich scarlet acid solution for 10 min. Subsequently, the tissue samples were first cleaned with distilled water, then stained for 10 min in phosphomolybdic-phosphotungstic acid solution and for 10 min in aniline blue solution. The samples were rinsed with distilled water and then incubated for 3 min in acetic acid. Finally, followed by dehydration with different concentrations of ethanol such as 100% ethanol in 3 min, 95% ethanol in 2 min, and followed 10 min in Xylene. The tissue slides were mounted with 1 drop of mounting medium. The collagen fibers production and collagen intensity were observed by microscope and quantified by ImageJ software.

Immunofluorescent staining. The tissue slices were deparaffinized and hydrated, and then the non-specific binding sites were blocked by adding 4% BSA in PBS at room temperature for an hour. Next, the sections were incubated with fist antibodies against vimentin, α-SMA, TNF, IL6, MCP-1, IL-1β, and Ki-67 overnight at 4˚C. After washing with PBS, the second antibody, Alexa Flour 488 goat anti-mouse, was incubated on the tissue sections in the dark for 1 h at RT, followed by nuclear labeling with 4',6-diamidino-2phenylindole (DAPI VECTASHIELD) for fluorescence imaging and keep at –20˚C. Imaging of the fluorescent signals was then performed using a confocal microscope. The images were analyzed using ImageJ software to measure the intensity of the above biomarkers, including inflammatory cytokines and proliferation.

ELISA. The wound tissues from control and chitosan groups on day 13 post-surgery were obtained and snap freeze in liquid nitrogen. The samples were homogenized in PROPREPTM Protein Extraction Solution and centrifuge at 14,000×*g* for 15 min at 4˚C to collect the supernatants. These protein solutions were used to assess TNF-, IL-6, IL-1, and MCP-1 cytokine expression levels in wound tissues by ELISA Kits following the manufacturer's suggested protocol.

Western blot analysis. The western blot experiment was conducted for α-SMA, collagen I, and TGF-β1 expression from the wound tissue in the proliferation phase. The protein was extracted as described above. A standard BCA method was used to determine protein concentration, and the protein samples were prepared for immunoblotting on a nitrocellulose membrane. After blocking with 5% nonfat dry skim milk, mouse anti-α-SMA, anti-GADPH mouse anti-collagen I, mouse anti-TGF-β1 were incubated with the membranes as primary antibodies at 4˚C overnight. After that, the secondary antibody, an (H+L)- HRP conjugate was used for 2 h. The protein expression levels were visualized by ChemiDoc™ Imaging System (Bio-Rad Laboratories) ImageJ program was used to test the expression of target proteins and normalized them to the beta-actin expression.

Determination of nitrite production in wound lysates. Nitrite and NO oxidation products in wound lysates were determined by using the Griess-modified reagent. A mix of 50 μl of 1× Griess-modified reagent and 50 μl of protein extract (30 mg/ml) was incubated at room temperature for 15 min. A series dilution of nitrite standard solutions was prepared 2-time dilution with ranges from 0 to 50 μM for a standard curve. The absorbance was measured at the wavelength of 504 nm.

Determination of cellular ROS production in wound lysates. The ROS production was performed by DCF-DA Kits. 30 mg/ml in 100 μl of protein extract from control and chitosan hydrocolloid groups containing 20 μM of DCF-DA solution was incubated at 37˚C, 5% CO_2 for 45 min in the dark. The fluorescence intensity was detected by fluorescence spectroscopy with excitation/emission at 485/535 nm.

MTT assay. Chitosan hydrocolloid was cut into 1.5 cm^2 and immersed in 15 ml of cell medium for 48 h for cell culture. An intensity of Raw 267.4 cells 6×10^4 well/cell was grown into a 24 well-plate for 24, and 48 h. The MTT assay method examined the vitality of non-treated and treated cells with Chitosan hydrocolloid. Briefly, cells were cultured with media supplementing 0.5 mg/ml MTT at 37˚C, 5% CO_2 for 4 h. After that, all media was taken out, and the plate was rinsed with 1x PBS. 200 μl of Dimethyl sulfoxide

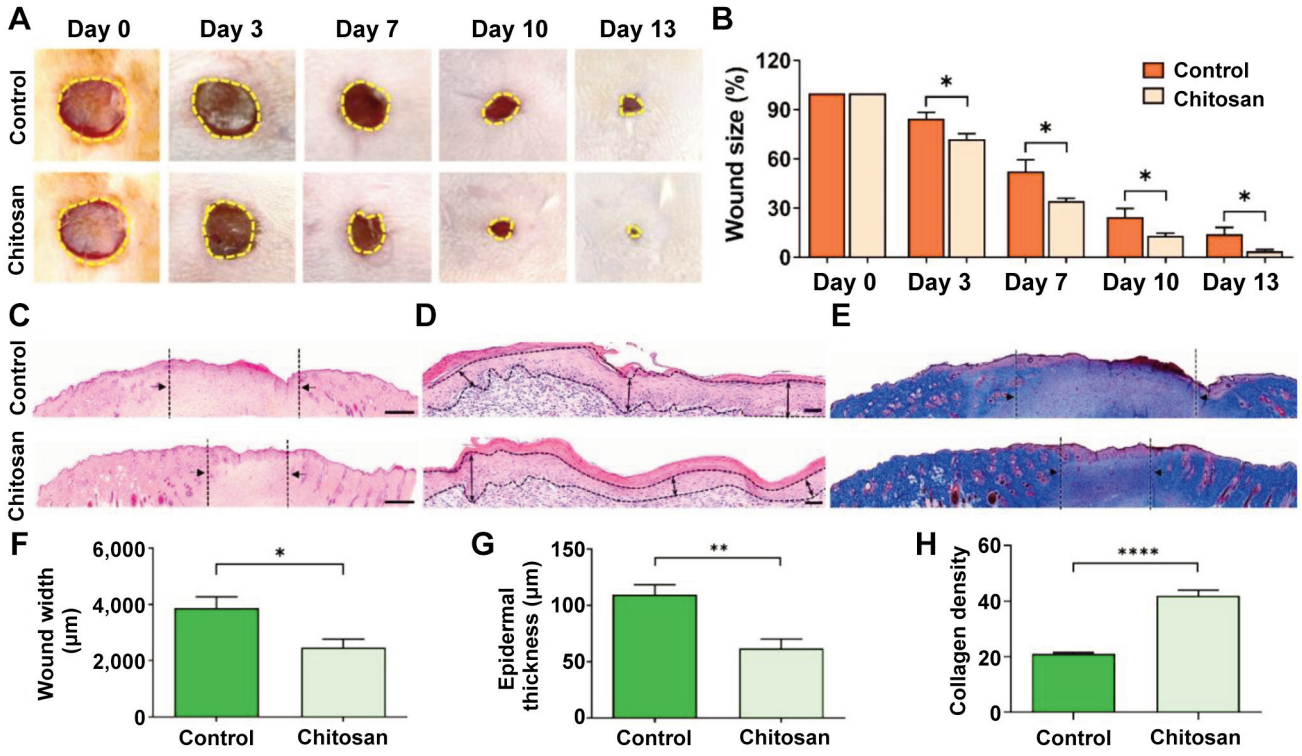

Figure 1. *Acceleration of wound healing by chitosan-embedded patch in rats. (A) Progressive visualization of wound healing with untreated chitosan embedded patch group (control) and treated chitosan embedded patch group (chitosan). (B) Progressive wound closure size. (C) Hematoxylin and eosin (H&E) staining of wound areas on day 13, scale bar 1,000 μm. (D) H&E staining of epidermal layers of wound areas on day 13, scale bar 50 μm. (E) Masson's trichrome (MT) staining of wound areas on day 13. (F) Quantitative wound width value of the control versus chitosan group on day 13. (G) Quantitative epidermis thickness gap of the control versus chitosan group on day 13. (H) Quantitative result of collagen density of the control versus chitosan group on day 13. The presented values are the experimental results on 6 rats for each group. Data are shown as the mean±SEM. *p≤0.05, **p≤0.005, ****p≤0.0001.*

was used to suspend the formazan product. Then, the absorbance was measured at 570 nm wavelength.

Statistical analysis. The data were displayed as mean value±standard of the mean bar from repeating three to five independent experiments using GraphPad Prism software and statistical analysis was performed by comparison between groups. A *p*-value less than 0.05 was considered statistically significant in the unpaired *t*-test.

Ethics statement. Institutional Review Board Statement: The animal study protocol was approved by Bundang Seoul National University Hospital's Institutional Animal Care and Use Committee (approval number: BA-1802-241-014-08).

Results

Macroscopic and microscopic visualization and observation of the wound healing process. The macroscopic images of wound healing on rats following day 0, day 3, day 7, day 10, and day 13 were captured and depicted as shown in Figure 1A. The figure displayed the decrease in wound size of other untreated groups (control group) and chitosan embedded patch treated group (chitosan group). However, there existed a faster rate of wound healing after day 3 in the chitosan group. Figure 1B demonstrates the quantitatively faster healing rate, with an obvious decrease in the wound size of the chitosan group compared to that of the control group from day 0 to day 13. The fresh epidermal and granulation tissues on day 13 were sectioned and performed H&E and MT staining to evaluate the microscopic alteration of the wound recovery of the control and chitosan groups, shown in Figure 1C-E. The cross-sectional analysis of H&E staining clearly represented a reduction in wound width of the chitosan group (2,449±318 μm) in comparison to those of the control group (3,965±398 μm) (Figure 1F). A significant increase in epidermal thickness was also observed, from the control group (61.9±8.3 μm) to the chitosan group (109.6±8.7 μm) (Figure 1G). In addition, the collagen formation was investigated by MT staining showing a significantly higher content of collagen deposition in chitosan-treated samples than those of the control ones by the intense and evenly distributed appearance of blue stains

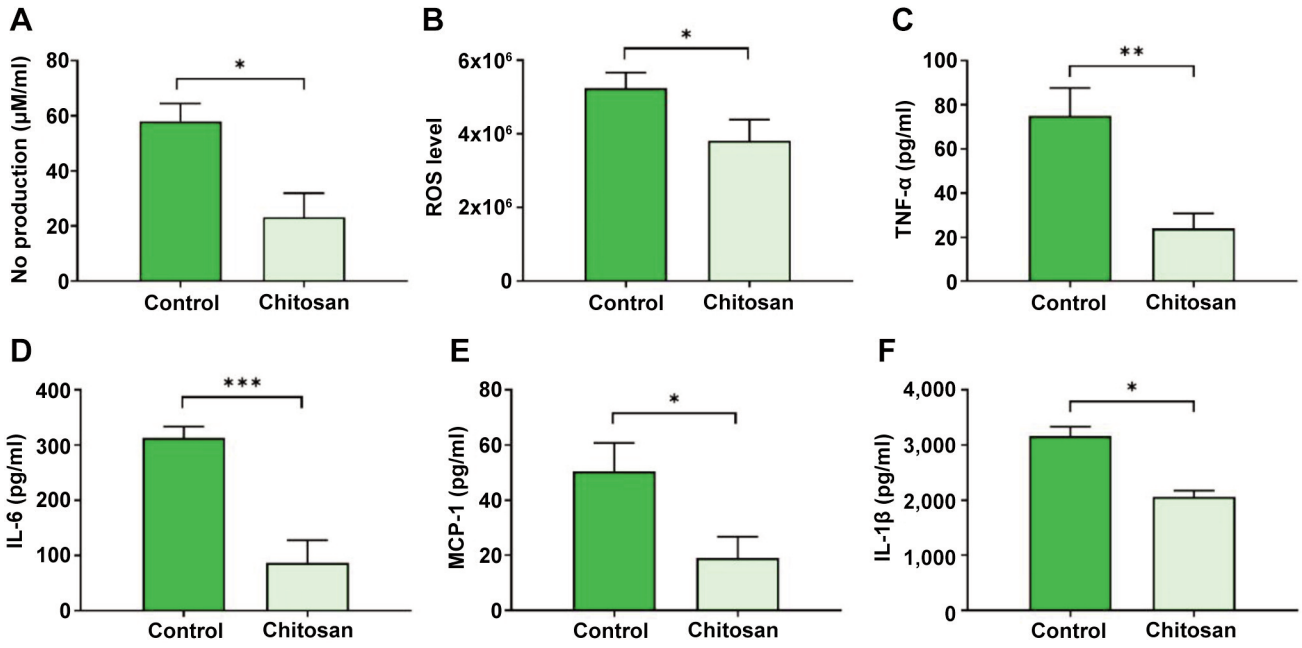

Figure 2. *Reduction of inflammatory response by the chitosan-embedded patch. Comparison of pro-inflammatory biomarkers expression extracted from wound areas on day 13, in which (A) Nitric oxide (NO) production by nitrate assay, (B) Reactive oxygen species (ROS) level by ROS assay, and (C) Tumor necrosis factor alpha (TNF-α), (D) Interleukin 6 (IL-6), (E) Monocyte chemoattractant protein 1 (MCP-1), (F) Interleukin 1 beta (IL-1β) by ELISA. The presented values are the experimental results on 6 rats for each group. Data are shown as the mean±SEM. *p≤0.05, **p≤0.005, ***p≤0.001.*

inside the models (Figure 1E). The statistically quantitative analysis of collagen formation exhibited the blue density of the chitosan group was approximately 41.9±1.9% which was more elevated than the value of the control group, 21.1±0.5% (Figure 1H).

Inflammatory phase acceleration and inflammatory response of the wound healing process. As shown in Figure 2A, the NO production level in the control group was elevated to 58±6.4 μM/ml, and the level of NO in the chitosan group was only 23.3±8.7 μM/ml. The reactive oxygen species (ROS) production level revealed a significant decrease in the chitosan group [$(3.81\pm0.6)\times10^6$] compared to the control group [$(5.24\pm0.4)\times10^6$] (Figure 2B). In addition, ELISA assays were performed when the healing process was completed (day 13) to evaluate and measure the expression of pro-inflammatory cytokines, which assessed the ability to ease inflammation of the chitosan-embedded patch (Figure 2C-F). In Figure 2C, the level of TNF-α remarkably declined in the chitosan group (24.0±6.7 pg/ml) compared to the control group (75.0±12.6 pg/ml). Additionally, a similar trend existed in the expression of IL-6, IL-1β, and MCP-1 (Figure 2D-F).

Immunofluorescence staining was conducted to elaborate further on the inflammatory acceleration and responses of pro-inflammatory cytokines in both the control and chitosan groups, as shown in Figure 3A-D. A quantitative analysis of staining results showed a significant decrease in pro-inflammatory cytokines intensity of the control group compared to that of the chitosan group, as shown in Figure 3E. Specifically, the intensity of TNF-α was 28.7±1.7 in the control group and decreased to 19.9±0.8 in the chitosan group. The intensity of IL-6 was 27.7±1.8 in the control group and also decreased to 13.7±1.1 in the chitosan group. The intensity of MCP-1 was 16.5±0.9 in the chitosan group, and significantly higher in the control group at 27.7±1.3. A similar trend was also observed in the intensity of IL-1β, in which the control group was 18.9±0.9 dropping to 13.9±0.6 for the chitosan group. Furthermore, M1 macrophage demonstrated by F4/80 and inducible nitric oxide synthase (iNOS) markers also presented significantly higher levels in the control group in comparison to the chitosan group (Figure 3F-H).

We examined the cytotoxicity of the chitosan-embedded patch to RAW 246.7 cell line in 24 and 48 h by using the MTT assay. For the chitosan group, the RAW cell was grown over time with incubation of the media secreted from the chitosan patches. The data showed a negligible change of OD intensity between the control and chitosan group in both 24- and 48-h samples, along with a considerable increase in

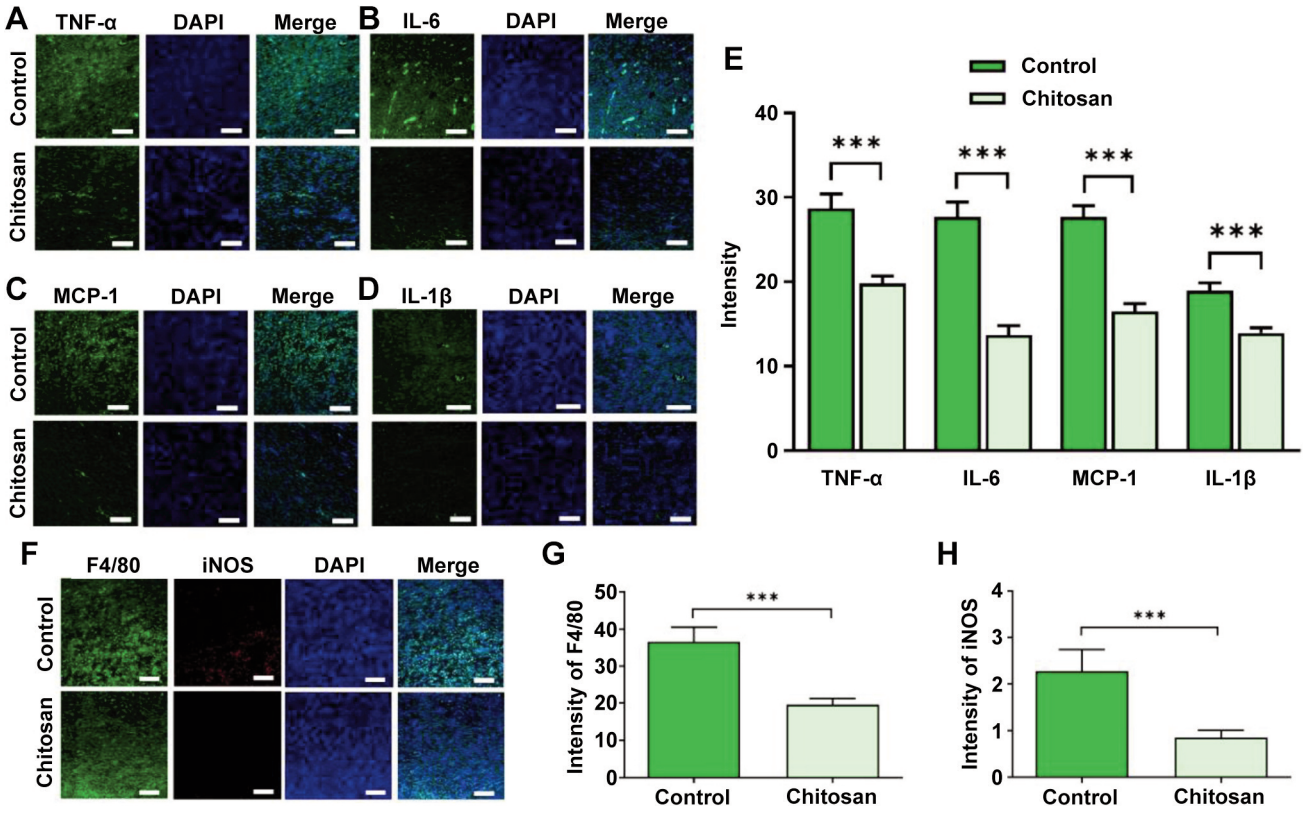

Figure 3. *Reduction of inflammatory response by the chitosan-embedded patch using immunofluorescence (IF) staining. IF staining results of biomarkers from wound areas on day 13, in which: (A) Tumor necrosis factor alpha (TNF-α), (B) Interleukin 6 (IL-6), (C) Monocyte chemoattractant protein 1 (MCP-1), and (D) Interleukin 1 beta (IL-1β). (E) Comparison of extracted fluorescent intensity of these biomarkers. (F) IF staining results of F4/80 and inducible nitric oxide synthase (iNOS) from wound areas on day 13. Comparison of extracted fluorescent intensity of (G) F4/80 and (H) iNOS. Scale bar=50 μm. The presented values are the experimental results on 6 rats for each group. Data are shown as the mean±SEM. ***p≤0.001.*

OD intensity from 24 h to 48 h, proving the non-toxicity of the chitosan patches (Figure 4A). To evaluate the immunogenic reactions *in vitro* and the capability of chitosan to suppress inflammation, we utilized lipopolysaccharides (LPS) as a pro-inflammatory reagent extracted by gram-negative bacteria to infect cells. We described the inflammatory responses in the four groups: control, LPS, chitosan hydrocolloid (chitosan HC) patch, and chitosan HC+LPS. The graphs in Figure 4B and C depicted concentrations of TNF-α and IL-6 in those treated conditions, respectively. Both of them showed an obvious increase when treated with LPS reflecting an effective inflammatory stimulation. In contrast, a positive effect of the chitosan HC could be observed as there was a decrease in the concentration of both these pro-inflammatory cytokines (*e.g.*, TNF-α and IL-6) in the (chitosan HC+LPS) groups compared to those in the LPS group. In addition to the chitosan HC patch, we also evaluated the anti-inflammatory of chitosan powder (chitosan P) by using 30 and 300 μg/ml chitosan low molecular weight to RAW 246.7 cell line (Figure 4D and E). The *in vitro* experiments with chitosan P displayed a similar incline toward the investigation with chitosan patch, providing further evidence for the inflammatory suppression ability of chitosan.

Proliferation phase acceleration and remodeling alteration of the wound healing process. To evaluate the proliferative acceleration of the chitosan-embedded patch, we employed immunofluorescence (IF) staining for various proliferation markers. The representative IF images shown in Figure 5A, C, and E correspond to vimentin, Ki67, and α-SMA, respectively. In Figure 5B, there displayed an unprecedented higher in the intensity of vimentin in the chitosan group, which was almost 30% as much as that of the control group. Moreover, other cell proliferation markers (*e.g.*, Ki67 and α-SMA) also demonstrated a statistically significant increase from the control group to the chitosan group, as shown in Figure 5D-F.

Furthermore, western blotting assays were performed to provide a comprehensive assessment of the proliferation

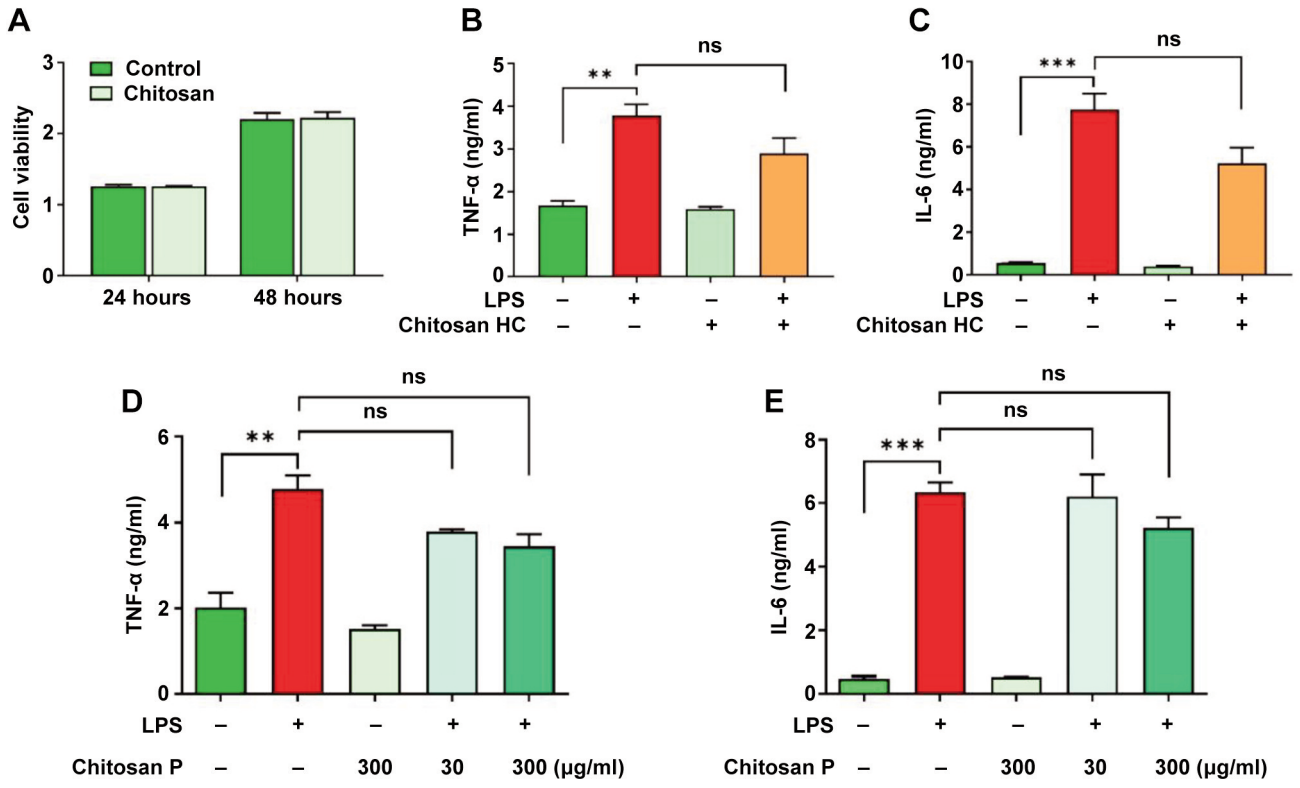

Figure 4. *Anti-inflammatory properties of the chitosan embedded patch and chitosan powder in RAW 246.7 cells. (A) Cytotoxicity evaluation on the chitosan embedded patch by 3-(4, 5-dimethylthiazolyl-2-2,5-diphenyltetrazolium bromide) (MTT) assay. ELISA results of (B) Tumor necrosis factor alpha (TNF-α) and (C) Interleukin 6 (IL-6) expressions in various conditions for our chitosan hydrocolloid (chitosan HC) patch. ELISA results of (D) TNF-α and (E) IL-6 expression in various conditions for chitosan powder (chitosan P). The presented values are the experimental results of 3 trials for each group. Data are shown as the mean±SEM. $^{ns}p>0.05$, $^{**}p\leq0.005$, $^{***}p\leq0.001$.*

phase. The result of the immunoblot assay of proteins presenting cell migration and differentiation was shown in Figure 6A. The western blotting results presented a considerable difference between the two groups of samples. Vimentin, α-SMA, collagen 1, and TGF-β1 were all expressed a higher level in the chitosan group in comparison to the control group (Figure 6B). Remarkably, we revealed a dramatic increase in expression of TGF-β1 (0.9571±0.1417), a marker that may reflect the capability of myoblast cells to stimulate tissue formation, in the chitosan group appearing almost 3.65 times as high as it in the control group (0.6069±0.1035). Furthermore, collagen formation during wound recovery, which manifests the remodeling occurrence of extracellular matrix in gowning tissue, was also demonstrated by a significant increase in collagen I protein expression in the chitosan group (Figure 6B).

In addition, M2 macrophages were chosen to access more insight into the proliferative aspects near the end of the wound healing process. These macrophages are anti-inflammatory factors that suppress the inflammatory process by secreting anti-inflammatory cytokines to the surrounding cellular environment. The analysis was conducted using IF staining of Agr1 and CD163 biomarkers, as shown in Figure 6C-E. According to the findings, the Agr1 and CD163 intensity significantly increased in the chitosan group compared to the control group (Figure 6D and E).

Discussion

Hemostasis, inflammation, proliferation, and remodeling are the four phases that occur sequentially throughout a wound healing process (26, 27). Since the remodeling phase in which scar formation occurs may take a few years, we focused on investigating the hemostasis, inflammation, and proliferation stages of wound healing which happen in a short time of injuries and surround most of the wound healing process.

The hemostasis process, along with the coagulation of blood clots around the wound scratches, was continuously observed in non-treated (control) and chitosan-embedded patch-treated (chitosan) groups (Figure 1). Starting from day 3, significant differences between wound areas, wound width

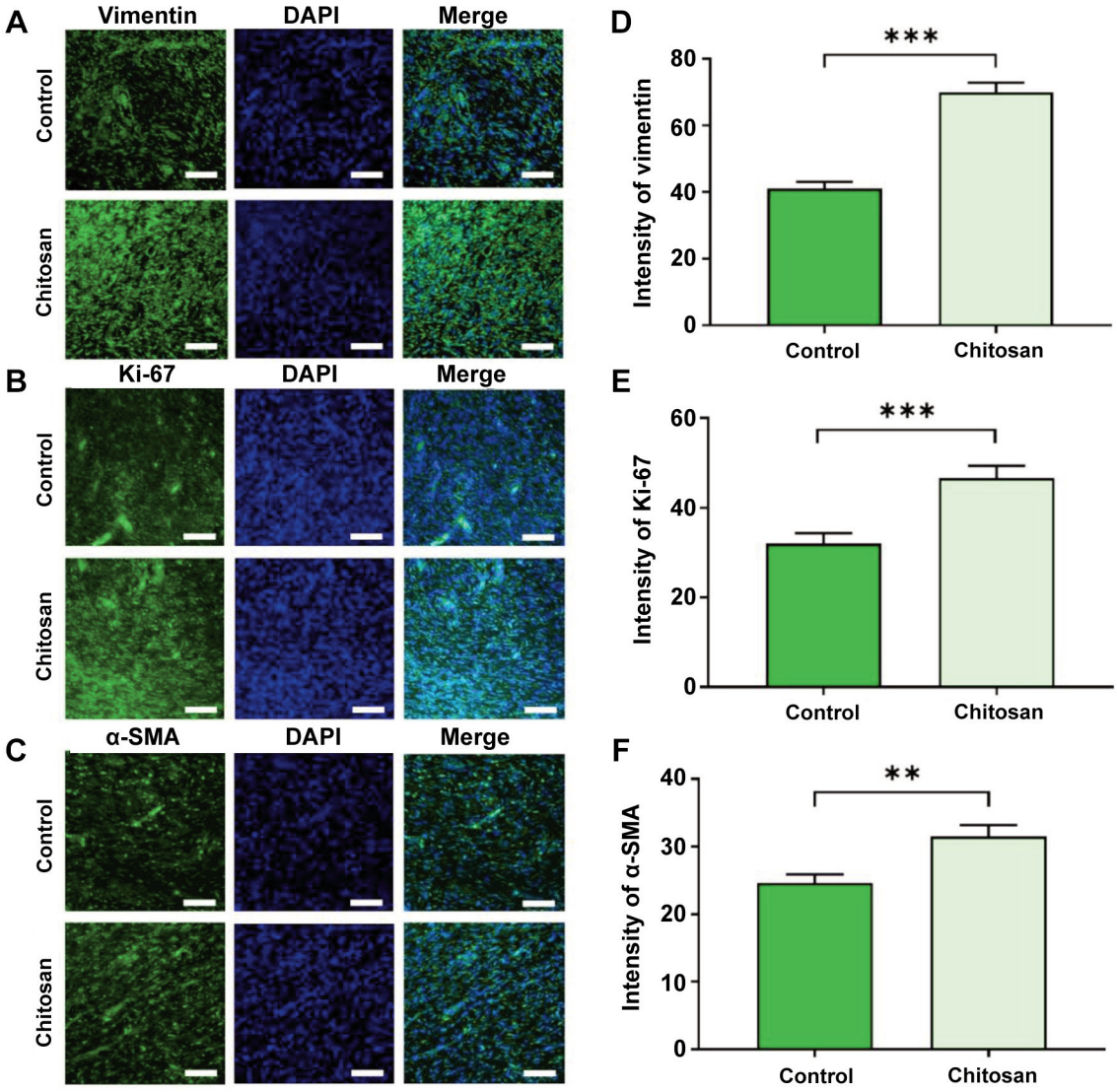

Figure 5. *Proliferative acceleration of wound healing by the chitosan-embedded patch. Immunofluorescence (IF) staining images of (A) Vimentin, (B) Ki-67, and (C) Alpha smooth muscle actin (α-SMA). Quantitative analysis of the fluorescent intensity of (D) Vimentin, (E) Ki-67, and (F) α-SMA. Scale bar=50 μm. The presented values are the experimental results on 6 rats for each group. Data are shown as the mean±SEM. **p≤0.005, ***p≤0.001.*

and epidermal thickness of the control and chitosan group suggested the dash ability to promote wound alteration of our product on rat model in a short period. Denser epidermal thickness and smaller wound width of the treated group indicated that wound reconstruction in that group was better than the control group. In addition to the wound morphology, collagen density in the treated group was also significantly higher than in the control group. These results suggested our chitosan-embedded patch promotes and supports intensely and effectively hemostasis during wound healing.

Nitric oxide (NO) displays a perspective wound reconstruction agent because of its capability to regulate and manage inflammation, cell proliferation, collagen deposition, and bacterial eradication (28-30). The activation of iNOS causes large amounts of NO to be generated in activated macrophages, promoting inflammation and defense against bacterial infections (31-33). The release of NO level in chitosan embedded patch treated group was remarkably lower than that of the control group, demonstrating a suppressive impact of chitosan embedded patch against the inflammation response during wound healing.

Reactive oxygen species (ROS) play a crucial role in triggering the immune response, attributing its function to immunity by regulating the secretion of pro-inflammatory

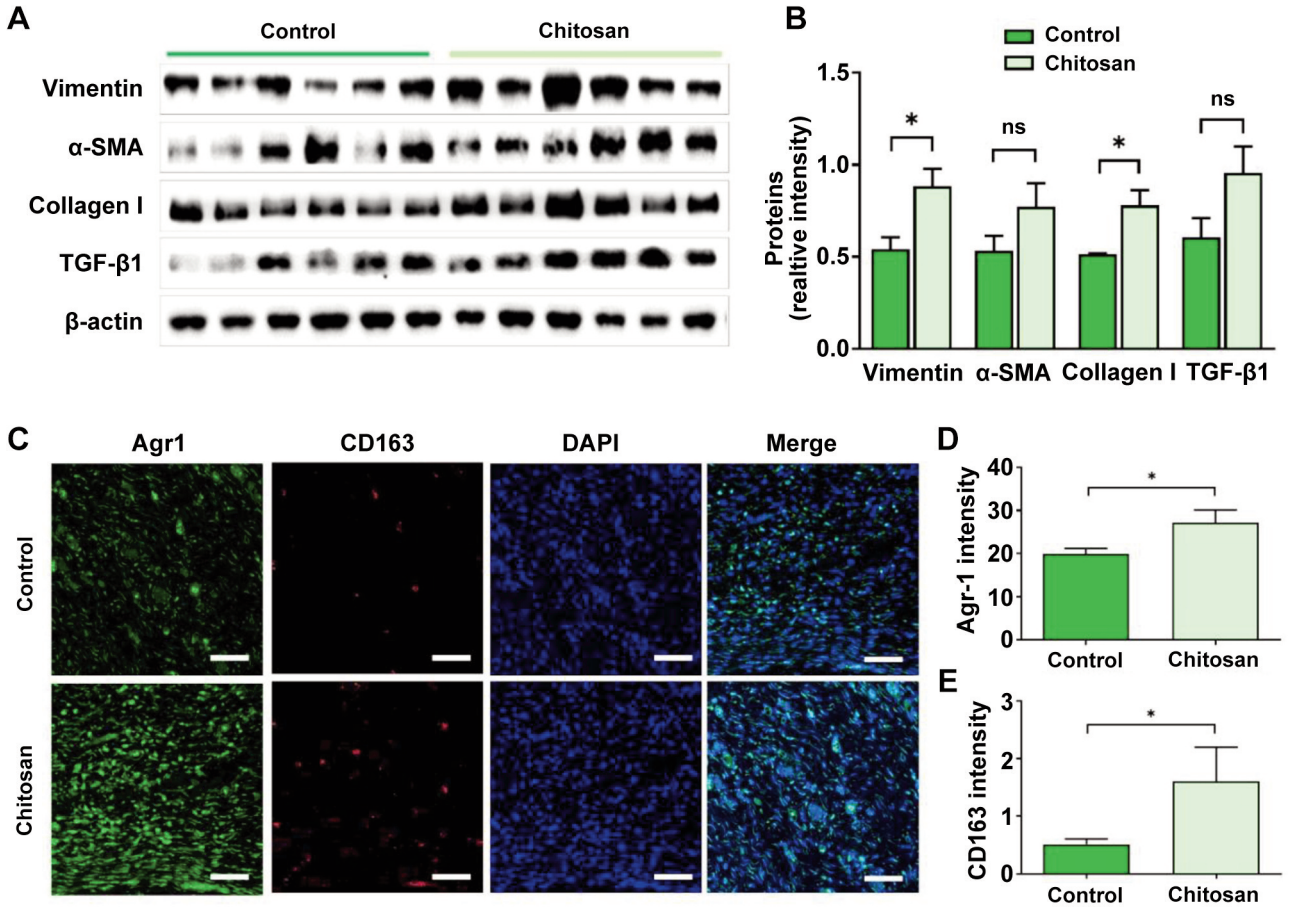

Figure 6. *Acceleration of wound healing by the chitosan-embedded patch. (A) Western blotting of proteins in wound areas on day 13. (B) Quantitative analysis of these proteins. (C) Immunofluorescence (IF) staining images of Arginase 1 (Agr1) and CD163 markers on day 13 wound areas. The quantitative intensity of (D) Agr1 and (E) CD163. Scale bar=50 μm. The presented values are the experimental results on 6 rats for each group. Data are shown as the mean±SEM.* $^{ns}p>0.05$, $*p<0.05$.

cytokines (34). ROS act as a signaling or mediator molecule depending on the level of ROS in the microenvironment. Elevated ROS levels result in inflammation due to the induction of oxidative stress that diminishes the antioxidant ability and damages the cell membrane and cellular components, leading to chronic impairment in cellular functions and further triggering apoptosis and necrosis (35, 36). In our study, the release of ROS in the chitosan group was significantly lower than in the control group, implying the ability to repress ROS production, which aided the inflammatory acceleration process.

Pro-inflammatory cytokines (*e.g.*, IL-6, TNF-α, IL-1β, and MCP-1) generally affect cell growth, proliferation, migration, and immune activation that carry immune signaling between cells during tissue repair (37, 38). However, overexpression of pro-inflammatory cytokines in cells may result in increased oxidative stress and deactivation of the epidermal proliferation of endothelial cells, which causes a permanent wound (39, 40). Appropriately, our ELISA results demonstrated a noticeable decline in pro-inflammatory cytokine release in chitosan-embedded patch-treated groups compared to the control group. When macrophages were activated by inflammatory factors surrounding the wound, iNOS expression increased, resulting in high levels of NO, TNF-α, and IL-6 (41, 42). In addition, immunofluorescence staining data represented an amplification in fluorescent signals of inflammatory cytokines in the control group, which contrast declined in the chitosan group, contributing shreds of evidence to the anti-inflammatory function of our chitosan-embedded patch. The data suggested the potential capability to alleviate pro-inflammatory cytokines to promote the sequential wound phase of our product.

Lipopolysaccharide (LPS) is an agent extracted from gram-negative bacteria and applied in various *in vitro* experiments to assess immunogenic reactions with

dramatically increase in the manifestation of pro-inflammatory cytokines (43, 44). In accordance with *in vivo* tests, the *in vitro* experiments demonstrated the anti-infection of chitosan in terms of "patch" and "powder" against LPS-induced inflammation in cells. The release of cytokines was downregulated in the LPS-induced group treated with chitosan embedded patch. Chitosan solution of 30 and 300 μg/ml in represented the same trend that the expression of inflammatory cytokines decreased when increasing chitosan concentration. As a result, both chitosan-embedded patches and chitosan powder showed a capacity of suspending *in vitro* cellular-induced inflammation, thus partially proving their ability against bacterial infection. Owning to the ease of use, the chitosan-embedded patches would be a potential product for wound healing treatments regarding anti-inflammation.

Fibroblast proliferation is one of the most critical factors in evaluating wound healing circulation, which is recruited during the expression of many growth factors (45, 46). Vimentin has been suggested to be involved in cell migration and extracellular matrix interaction, which is highlighted in fibroblast proliferation in wound healing (47, 48). Vimentin thus controls cell-adhesion development, maturity, and adhesive ability, allowing cells to adjust their connection to collagen, and manage the growth of cell expansion and its movement through connective tissues (49-51). Our data (*e.g.*, IF staining and western blotting) demonstrated a higher expression of vimentin in the chitosan patch-treated group than in the control groups, indicating the cascade of fibroblast migration cultivates ECM after wound recovery.

Though the release of transforming growth factor-β1 (TGF-β1) may exaggerate extracellular matrix formation leading to scar formation, it has been considered a principal factor in evaluating wound healing due to its competencies in activation, migration, and proliferation of fibroblasts to occlude a wound (52, 53). Transformation of fibroblast to contractile myofibroblast (activated form) results in the formation of granulation tissue ascribed to the release of TGF-β1, thus causing the release of alpha-smooth muscle actin (α-SMA) (54, 55). In this study, western blotting data demonstrated a considerable increase in TGF-β1 content, thus leading to the rise in contractile α-SMA in the chitosan-embedded patch-treated group compared to that of the control group. The data in both IF staining and Western blot of growth factors complemented each other and accentuated the success of our product in cultivating wound recovery.

Fibroblasts ascribe to collagen deposition, which degrades in the initial state of an injury to regulate pro-inflammatory cytokines later on signals and promotes fibroblast proliferation and angiogenesis (56, 57). In addition, collagen is a complex macromolecule that constitutes the ECM and facilitates the process of tissue regeneration and repair (58, 59). Herein, there was a great incline in the content of collagen I in the chitosan group compared to that of the control group (Figure 6B). As a result, it could be concluded that our chitosan patch product significantly impacted invigorating cell migration onto the wound to achieve a practical proliferation stage, repairing ECM to support granulation tissue formation.

Macrophages are critical participants in wound recovery as they supply provisional signaling molecules engaging in the proliferative phase of the healing process (60, 61). Macrophages can be classified as M1-type and M2-type depending on their activation state and function (62). M1 macrophages are considered to secrete pro-inflammatory cytokines participating in the immune response to accelerate the inflammation phase (63). In contrast, M2 macrophages are activated in the proliferative phase to release anti-inflammatory cytokines and growth factors to promote tissue repair (64). The significant decline of F4/80, a marker of M1 macrophages, and a remarkable rise in the intensity of CD163, a marker of M2 macrophages, in the chitosan group clarified the competency to refrain from inflammation and promote the spread and migration of fibroblast cells to reconstruct the ECM.

Conclusion

In conclusion, we evaluated the ability of our chitosan-embedded patch to promote wound healing, which was presented by the suppression of pro-inflammatory cytokines along with the increase in proliferative biomarker content. Specifically, a set of biomarkers including pro-inflammatory cytokines was investigated regarding protein concentration by western blotting, optical density by ELISA, and fluorescence density by IF staining, confirming the positive impact of the chitosan-embedded patch on accelerating the inflammatory phase. In addition, our chitosan patch attenuated oxidative stress by lowering the level of ROS and NO in the treated group, which triggers cell protection and skin regeneration in the proliferation stage. Furthermore, we also demonstrated the capability of the chitosan patch in promoting proliferation completion, elaborated by the elevation in activated fibroblast growth *via* signals of vimentin, Ki-67, and α-SMA markers. As a result, extracellular matrix (ECM) was induced to recover, as observed by ECM markers such as collagen I and TGF-β1, as well as M2 macrophage recruitment enhancement. Our study on the chitosan-based hydrocolloid patch not only provides an effective product for skin wound healing, but also contributes to understanding the mechanisms for future wound healing product development.

Conflicts of Interest

The Authors declare that they have no competing financial interest.

Authors' Contributions

Le Thi Thuy Linh, Nguyen Ngan Giang, Pham Ngoc Chien, Sun-Young Nam, Chan-Yeong Heo: Conceptualization, methodology, writing original draft and editing. Xin Rui Zhang, Nguyen Van Long, Le Thi Van Anh, Pham Thi Nga: Software, visualization. Sun-Young Nam, Chan-Yeong Heo: Supervision, validation, project administration.

Acknowledgements

This research was funded by grant No. 14-2015-0008 from SNUBH Research Fund and by a grand of the Korea Health Technology R&D Project through the Korea Health Industry Development Institute (KHIDI), funded by the Ministry of Health & Welfare, Republic of Korea (grant number: HR22C1363), and by the Development of new products subject to purchase conditions (S2942288) funded by the Ministry of SMEs and Startups (MSS, Korea).

References

1 Martin P: Wound healing—aiming for perfect skin regeneration. Science *276(5309)*: 75-81, 1997. PMID: 9082989. DOI: 10.1126/science.276.5309.75

2 Takeo M, Lee W and Ito M: Wound healing and skin regeneration. Cold Spring Harb Perspect Med *5(1)*: a023267, 2015. PMID: 25561722. DOI: 10.1101/cshperspect.a023267

3 Park YJ and Lee HK: The role of skin and orogenital microbiota in protective immunity and chronic immune-mediated inflammatory disease. Front Immunol *8*: 1955, 2018. PMID: 29375574. DOI: 10.3389/fimmu.2017.01955

4 Wilkinson HN and Hardman MJ: Wound healing: cellular mechanisms and pathological outcomes. Open Biol *10(9)*: 200223, 2020. PMID: 32993416. DOI: 10.1098/rsob.200223

5 Trinh XT, Long NV, Van Anh LT, Nga PT, Giang NN, Chien PN, Nam SY and Heo CY: A comprehensive review of natural compounds for wound healing: Targeting bioactivity perspective. Int J Mol Sci *23(17)*: 9573, 2022. PMID: 36076971. DOI: 10.3390/ijms23179573

6 Barootchi S, Tavelli L, Gianfilippo RD, Eber R, Stefanini M, Zucchelli G and Wang HL: Acellular dermal matrix for root coverage procedures: 9-year assessment of treated isolated gingival recessions and their adjacent untreated sites. J Periodontol *92(2)*: 254-262, 2021. PMID: 32729954. DOI: 10.1002/JPER.20-0310

7 Sood A, Granick MS and Tomaselli NL: Wound dressings and comparative effectiveness data. Adv Wound Care (New Rochelle) *3(8)*: 511-529, 2014. PMID: 25126472. DOI: 10.1089/wound.2012.0401

8 Zhang M and Zhao X: Alginate hydrogel dressings for advanced wound management. Int J Biol Macromol *162*: 1414-1428, 2020. PMID: 32777428. DOI: 10.1016/j.ijbiomac.2020.07.311

9 Shi C, Wang C, Liu H, Li Q, Li R, Zhang Y, Liu Y, Shao Y and Wang J: Selection of appropriate wound dressing for various wounds. Front Bioeng Biotechnol *8*: 182, 2020. PMID: 32266224. DOI: 10.3389/fbioe.2020.00182

10 Weller C, Weller C and Team V: Interactive dressings and their role in moist wound management. Advanced Textiles for Wound Care: 105-134, 2020. DOI: 10.1016/B978-0-08-102192-7.00004-7

11 Liang Y, Liang Y, Zhang H and Guo B: Antibacterial biomaterials for skin wound dressing. Asian J Pharm Sci *17(3)*: 353-384, 2022. PMID: 35782328. DOI: 10.1016/j.ajps.2022.01.001

12 Mahyudin F, Edward M, Basuki M, Basrewan Y and Rahman A: Modern and classic wound dressing comparison in wound healing, comfort and cost. Jurnal Ners *15(1)*: 31-36, 2022. DOI: 10.20473/jn.v15i1.16597

13 Brumberg V, Astrelina T, Malivanova T and Samoilov A: Modern wound dressings: Hydrogel dressings. Biomedicines *9(9)*: 1235, 2021. PMID: 34572421. DOI: 10.3390/biomedicines9091235

14 Weller CD, Team V and Sussman G: First-line interactive wound dressing update: a comprehensive review of the evidence. Front Pharmacol *11*: 155, 2020. PMID: 32180720. DOI: 10.3389/fphar.2020.00155

15 Laurano R, Boffito M, Ciardelli G and Chiono V: Wound dressing products: A translational investigation from the bench to the market. Engineered Regeneration *3(2)*: 182-200, 2023. DOI: 10.1016/j.engreg.2022.04.002

16 Deng C, He L, Zhao M, Yang D and Liu Y: Biological properties of the chitosan-gelatin sponge wound dressing. Carbohydrate Polymers *69(3)*: 583-589, 2019. DOI: 10.1016/j.carbpol.2007.01.014

17 Periayah MH, Halim AS, Hussein AR, Saad AZ, Rashid AH and Noorsal K: *In vitro* capacity of different grades of chitosan derivatives to induce platelet adhesion and aggregation. Int J Biol Macromol *52*: 244-249, 2013. PMID: 23063426. DOI: 10.1016/j.ijbiomac.2012.10.001

18 Acheson EM, Kheirabadi BS, Deguzman R, Dick EJ Jr and Holcomb JB: Comparison of hemorrhage control agents applied to lethal extremity arterial hemorrhages in swine. J Trauma *59(4)*: 865-74; discussion 874-5, 2005. PMID: 16374275. DOI: 10.1097/01.ta.0000187655.63698.9f

19 Kassem A, Ayoub GM and Malaeb L: Antibacterial activity of chitosan nano-composites and carbon nanotubes: A review. Sci Total Environ *668*: 566-576, 2019. PMID: 30856567. DOI: 10.1016/j.scitotenv.2019.02.446

20 Kakaei S and Shahbazi Y: Effect of chitosan-gelatin film incorporated with ethanolic red grape seed extract and Ziziphora clinopodioides essential oil on survival of Listeria monocytogenes and chemical, microbial and sensory properties of minced trout fillet. LWT - Food Science and Technology *72*: 432-438, 2021. DOI: 10.1016/j.lwt.2016.05.021

21 Nowzari F, Shábanpour B and Ojagh SM: Comparison of chitosan-gelatin composite and bilayer coating and film effect on the quality of refrigerated rainbow trout. Food Chem *141(3)*: 1667-1672, 2013. PMID: 23870876. DOI: 10.1016/j.foodchem.2013.03.022

22 Goy R, Britto D and Assis O: A review of the antimicrobial activity of chitosan. Polímeros *19(3)*: 241-247, 2019. DOI: 10.1590/s0104-14282009000300013

23 Eltahlawy K, Elbendary M, Elhendawy A and Hudson S: The antimicrobial activity of cotton fabrics treated with different crosslinking agents and chitosan. Carbohydrate Polymers *60(4)*: 421-430, 2019. DOI: 10.1016/j.carbpol.2005.02.019

24 Champer J, Patel J, Fernando N, Salehi E, Wong V and Kim J: Chitosan against cutaneous pathogens. AMB Express *3(1)*: 37, 2013. PMID: 23829873. DOI: 10.1186/2191-0855-3-37

25 Howling GI, Dettmar PW, Goddard PA, Hampson FC, Dornish M and Wood EJ: The effect of chitin and chitosan on the proliferation of human skin fibroblasts and keratinocytes *in vitro*. Biomaterials *22(22)*: 2959-2966, 2001. PMID: 11575470. DOI: 10.1016/s0142-9612(01)00042-4

26 Rodrigues M, Kosaric N, Bonham CA and Gurtner GC: Wound healing: a cellular perspective. Physiol Rev *99(1)*: 665-706, 2019. PMID: 30475656. DOI: 10.1152/physrev.00067.2017

27 Kita A, Saito Y, Miura N, Miyajima M, Yamamoto S, Sato T, Yotsuyanagi T, Fujimiya M and Chikenji TS: Altered regulation of mesenchymal cell senescence in adipose tissue promotes pathological changes associated with diabetic wound healing. Commun Biol *5(1)*: 310, 2022. PMID: 35383267. DOI: 10.1038/s42003-022-03266-3

28 Malone-Povolny MJ, Maloney SE and Schoenfisch MH: Nitric oxide therapy for diabetic wound healing. Adv Healthc Mater *8(12)*: e1801210, 2019. PMID: 30645055. DOI: 10.1002/adhm.201801210

29 Wu M, Lu Z, Wu K, Nam C, Zhang L and Guo J: Recent advances in the development of nitric oxide-releasing biomaterials and their application potentials in chronic wound healing. J Mater Chem B *9(35)*: 7063-7075, 2021. PMID: 34109343. DOI: 10.1039/d1tb00847a

30 Ahmed R, Augustine R, Chaudhry M, Akhtar UA, Zahid AA, Tariq M, Falahati M, Ahmad IS and Hasan A: Nitric oxide-releasing biomaterials for promoting wound healing in impaired diabetic wounds: State of the art and recent trends. Biomed Pharmacother *149*: 112707, 2022. PMID: 35303565. DOI: 10.1016/j.biopha.2022.112707

31 Xue Q, Yan Y, Zhang R and Xiong H: Regulation of iNOS on immune cells and its role in diseases. Int J Mol Sci *19(12)*: 3805, 2018. PMID: 30501075. DOI: 10.3390/ijms19123805

32 Mühl H, Bachmann M and Pfeilschifter J: Inducible NO synthase and antibacterial host defence in times of Th17/Th22/T22 immunity. Cell Microbiol *13(3)*: 340-348, 2011. PMID: 21199257. DOI: 10.1111/j.1462-5822.2010.01559.x

33 Lu G, Zhang R, Geng S, Peng L, Jayaraman P, Chen C, Xu F, Yang J, Li Q, Zheng H, Shen K, Wang J, Liu X, Wang W, Zheng Z, Qi CF, Si C, He JC, Liu K, Lira SA, Sikora AG, Li L and Xiong H: Myeloid cell-derived inducible nitric oxide synthase suppresses M1 macrophage polarization. Nat Commun *6*: 6676, 2015. PMID: 25813085. DOI: 10.1038/ncomms7676

34 Yang Z, Min Z and Yu B: Reactive oxygen species and immune regulation. Int Rev Immunol *39(6)*: 292-298, 2020. PMID: 32423322. DOI: 10.1080/08830185.2020.1768251

35 Herb M and Schramm M: Functions of ROS in macrophages and antimicrobial immunity. Antioxidants (Basel) *10(2)*: 313, 2021. PMID: 33669824. DOI: 10.3390/antiox10020313

36 Checa J and Aran JM: Reactive oxygen species: Drivers of physiological and pathological processes. J Inflamm Res *13*: 1057-1073, 2020. PMID: 33293849. DOI: 10.2147/JIR.S275595

37 Kany S, Vollrath JT and Relja B: Cytokines in inflammatory disease. Int J Mol Sci *20(23)*: 6008, 2019. PMID: 31795299. DOI: 10.3390/ijms20236008

38 Molnar V, Matišić V, Kodvanj I, Bjelica R, Jeleč Ž, Hudetz D, Rod E, Čukelj F, Vrdoljak T, Vidović D, Starešinić M, Sabalić S, Dobričić B, Petrović T, Antičević D, Borić I, Košir R, Zmrzljak UP and Primorac D: Cytokines and chemokines involved in osteoarthritis pathogenesis. Int J Mol Sci *22(17)*: 9208, 2021. PMID: 34502117. DOI: 10.3390/ijms22179208

39 Saha S, Buttari B, Panieri E, Profumo E and Saso L: An overview of Nrf2 signaling pathway and its role in inflammation. Molecules *25(22)*: 5474, 2020. PMID: 33238435. DOI: 10.3390/molecules25225474

40 Hsu T, Nguyen-Tran HH and Trojanowska M: Active roles of dysfunctional vascular endothelium in fibrosis and cancer. J Biomed Sci *26(1)*: 86, 2019. PMID: 31656195. DOI: 10.1186/s12929-019-0580-3

41 Wang LX, Zhang SX, Wu HJ, Rong XL and Guo J: M2b macrophage polarization and its roles in diseases. J Leukoc Biol *106(2)*: 345-358, 2019. PMID: 30576000. DOI: 10.1002/JLB.3RU1018-378RR

42 Das LM, Rosenjack J, Au L, Galle PS, Hansen MB, Cathcart MK, McCormick TS, Cooper KD, Silverstein RL and Lu KQ: Hyper-inflammation and skin destruction mediated by rosiglitazone activation of macrophages in IL-6 deficiency. J Invest Dermatol *135(2)*: 389-399, 2015. PMID: 25184961. DOI: 10.1038/jid.2014.375

43 Mbongue J, Vanterpool E, Firek A and Langridge W: Lipopolysaccharide-induced immunological tolerance in monocyte-derived dendritic cells. Immuno *2(3)*: 482-500, 2023. DOI: 10.3390/immuno2030030

44 Liu X, Yin S, Chen Y, Wu Y, Zheng W, Dong H, Bai Y, Qin Y, Li J, Feng S and Zhao P: LPS induced proinflammatory cytokine expression in human airway epithelial cells and macrophages *via* NF κB, STAT3 or AP 1 activation. Mol Med Rep *17(4)*: 5484-5491, 2018. PMID: 29393460. DOI: 10.3892/mmr.2018.8542

45 Addis R, Cruciani S, Santaniello S, Bellu E, Sarais G, Ventura C, Maioli M and Pintore G: Fibroblast proliferation and migration in wound healing by phytochemicals: evidence for a novel synergic outcome. Int J Med Sci *17(8)*: 1030-1042, 2020. PMID: 32410832. DOI: 10.7150/ijms.43986

46 Darby IA and Hewitson TD: Fibroblast differentiation in wound healing and fibrosis. Int Rev Cytol *257*: 143-179, 2007. PMID: 17280897. DOI: 10.1016/S0074-7696(07)57004-X

47 Battaglia RA, Delic S, Herrmann H and Snider NT: Vimentin on the move: new developments in cell migration. F1000Res *7(F1000 Faculty Rev)*: 1796, 2018. PMID: 30505430. DOI: 10.12688/f1000research.15967.1

48 Paulin D, Lilienbaum A, Kardjian S, Agbulut O and Li Z: Vimentin: Regulation and pathogenesis. Biochimie *197*: 96-112, 2022. PMID: 35151830. DOI: 10.1016/j.biochi.2022.02.003

49 Swoger M, Gupta S, Charrier EE, Bates M, Hehnly H and Patteson AE: Vimentin intermediate filaments mediate cell morphology on viscoelastic substrates. ACS Appl Bio Mater *5(2)*: 552-561, 2022. PMID: 34995457. DOI: 10.1021/acsabm.1c01046

50 Bandzerewicz A and Gadomska-Gajadhur A: Into the tissues: Extracellular matrix and its artificial substitutes: Cell signalling mechanisms. Cells *11(5)*: 914, 2022. PMID: 35269536. DOI: 10.3390/cells11050914

51 Biggs LC, Kim CS, Miroshnikova YA and Wickström SA: Mechanical forces in the skin: roles in tissue architecture, stability, and function. J Invest Dermatol *140(2)*: 284-290, 2020. PMID: 31326398. DOI: 10.1016/j.jid.2019.06.137

52 Peterson JM, Jay JW, Wang Y, Joglar AA, Prasai A, Palackic A, Wolf SE and El Ayadi A: Galunisertib exerts antifibrotic effects on TGF-β-induced fibroproliferative dermal fibroblasts. Int J Mol Sci *23(12)*: 6689, 2022. PMID: 35743131. DOI: 10.3390/ijms23126689

53 Liarte S, Bernabé-García Á and Nicolás FJ: Role of TGF-β in skin chronic wounds: a keratinocyte perspective. Cells *9(2)*: 306, 2020. PMID: 32012802. DOI: 10.3390/cells9020306

54 Tai Y, Woods EL, Dally J, Kong D, Steadman R, Moseley R and Midgley AC: Myofibroblasts: Function, formation, and scope of molecular therapies for skin fibrosis. Biomolecules *11(8)*: 1095, 2021. PMID: 34439762. DOI: 10.3390/biom11081095

55 Szóstek-Mioduchowska AZ, Lukasik K, Skarzynski DJ and Okuda K: Effect of transforming growth factor -β1 on α-smooth muscle actin and collagen expression in equine endometrial fibroblasts. Theriogenology *124*: 9-17, 2019. PMID: 30321755. DOI: 10.1016/j.theriogenology.2018.10.005

56 Chowdhury A, Nosoudi N, Karamched S, Parasaram V and Vyavahare N: Polyphenol treatments increase elastin and collagen deposition by human dermal fibroblasts; Implications to improve skin health. J Dermatol Sci *102(2)*: 94-100, 2021. PMID: 33766446. DOI: 10.1016/j.jdermsci.2021.03.002

57 Edgar S, Hopley B, Genovese L, Sibilla S, Laight D and Shute J: Effects of collagen-derived bioactive peptides and natural antioxidant compounds on proliferation and matrix protein synthesis by cultured normal human dermal fibroblasts. Sci Rep *8(1)*: 10474, 2018. PMID: 29992983. DOI: 10.1038/s41598-018-28492-w

58 Barbalinardo M, Biagetti M, Valle F, Cavallini M, Falini G and Montroni D: Green biocompatible method for the synthesis of collagen/chitin composites to study their composition and assembly influence on fibroblasts growth. Biomacromolecules *22(8)*: 3357-3365, 2021. PMID: 34278777. DOI: 10.1021/acs.biomac.1c00463

59 Winkler J, Abisoye-Ogunniyan A, Metcalf KJ and Werb Z: Concepts of extracellular matrix remodelling in tumour progression and metastasis. Nat Commun *11(1)*: 5120, 2020. PMID: 33037194. DOI: 10.1038/s41467-020-18794-x

60 Kotwal GJ and Chien S: Macrophage differentiation in normal and accelerated wound healing. Results Probl Cell Differ *62*: 353-364, 2017. PMID: 28455716. DOI: 10.1007/978-3-319-54090-0_14

61 Minutti CM, Knipper JA, Allen JE and Zaiss DM: Tissue-specific contribution of macrophages to wound healing. Semin Cell Dev Biol *61*: 3-11, 2017. PMID: 27521521. DOI: 10.1016/j.semcdb.2016.08.006

62 Arora S, Dev K, Agarwal B, Das P and Syed MA: Macrophages: Their role, activation and polarization in pulmonary diseases. Immunobiology *223(4-5)*: 383-396, 2018. PMID: 29146235. DOI: 10.1016/j.imbio.2017.11.001

63 Hu F, Lou N, Jiao J, Guo F, Xiang H and Shang D: Macrophages in pancreatitis: Mechanisms and therapeutic potential. Biomed Pharmacother *131*: 110693, 2020. PMID: 32882586. DOI: 10.1016/j.biopha.2020.110693

64 Sapudom J, Karaman S, Mohamed WKE, Garcia-Sabaté A, Quartey BC and Teo JCM: 3D *in vitro* M2 macrophage model to mimic modulation of tissue repair. NPJ Regen Med *6(1)*: 83, 2021. PMID: 34848722. DOI: 10.1038/s41536-021-00193-5

Received February 14, 2023
Revised March 2, 2023
Accepted March 21, 2023